Desalination and Water Treatment
www.deswater.com
doi: 10.1080/19443994.2015.1031187

57 (2016) 7841–7846
April

Taylor & Francis
Taylor & Francis Group

Enhanced removal of phosphate by hydrocalumite: synergism of $AlPO_4$ and $CaHPO_4{\cdot}2H_2O$ precipitation

Yongsheng Lu, Hetian Hou, Jun Zhao, Jizhi Zhou, Jianyong Liu, Linlin Feng, Guangren Qian, Yunfeng Xu*

School of Environmental and Chemical Engineering, Shanghai University, Shanghai 200444, China, emails: luys7174@shu.edu.cn (Y. Lu), hnn2246@163.com (H. Hou), junzhao@shu.edu.cn (J. Zhao), jizhi.zhou@shu.edu.cn (J. Zhou), liujianyong@shu.edu.cn (J. Liu), 276039084@qq.com (L. Feng), grqian@shu.edu.cn (G. Qian), Tel. +86 21 66137745; Fax: +86 21 66137761; email: yfxu@shu.edu.cn (Y. Xu)

Received 13 December 2014; Accepted 15 March 2015

ABSTRACT

In this work, the species of the precipitate after P removal in the solution was investigated. The characterization of calcined precipitates indicated that $CaHPO_4{\cdot}2H_2O$ (DCPD) and $AlPO_4$ were the predominant phosphorous precipitates at pH 5.0; the phosphorous removal was attributed to the formation of $Ca_5(PO_4)_3OH$ (HAP) at pH 11.0. Additionally, $AlPO_4$, DCPD, and HAP were formed in the neutral condition. This revealed that both Ca and Al in hydrocalumite were responsible for P removal. Correspondingly, based on the composition analysis, the molar ratio of (Ca + Al)/P in the extractable phosphorous precipitates increased from 1.05 to 2.21 with the increasing pH values. The results demonstrated that the phosphorous removal efficiency was reduced as the species evolution of Ca and Al precipitates. This work therefore proposed that lower pH promoted the phosphorous removal efficiency by Ca and Al consumption in LDH.

Keywords: Hydrocalumite; Phosphate; Chemical extraction; Structure evolution

1. Introduction

Phosphate, among the elements resulting in eutrophication, attracts much attention as an excess amount of phosphate (P), even at 0.5 mg/L, can lead to abundant development of aquatic plants, growth of algae, and destruction of the ecosystem in the water [1,2]. In order to effectively remove P from the P-contaminated waters, chemicals such as aluminum, iron, and calcium salts are most commonly used [3–5]. Generally, there are two mechanisms involved in this chemical treatment of phosphate, named the coagulation/adsorption of aluminum (iron) hydroxide and the precipitation of metal phosphates (aluminum phosphate, iron phosphate, or hydroxyapatite ($Ca_5(PO_4)_3OH$, HAP) [6–8].

In order to get a better P removal, hydrocalumite (Ca_2Al–Cl–LDH, $Ca_4Al_2(OH)_{12}Cl_2{\cdot}4H_2O$) has been introduced. Recently, our group has found that the maximum removal amount of P on Ca_2Al–Cl–LDH

*Corresponding author.

Presented at the 7th International Conference on Challenges in Environmental Science and Engineering (CESE 2014) 12–16 October 2014, Johor Bahru, Malaysia

was 135 mg P/g [9,10], the high removal efficiency of phosphate was contributed to the dissolution–reprecipitation process after the complete dissolution of the LDH [11,12]. Additionally, Ca- and Al-phosphate were predominant precipitates responsible for removal of P by Ca_2Al–Cl–LDH. These species of precipitates were influenced firmly by pH and initial concentration of P. Based on this principle, multistep treatment process were proposed for phosphate removal from high-concentration phosphate wastewater, in which $Ca_5(PO_4)_3OH$ (HAP) was produced at high pH, brushite (DCPD, $CaHPO_4{\cdot}2H_2O$) and $AlPO_4$ were formed at low pH [13]. This led to the increase of phosphate removal amount due to the high Ca and Al consuming efficiency.

However, in batch experiments, Al-phosphate precipitate was supposed to be a poor-crystallized $AlPO_4$ that could not be well identified via X-ray diffraction (XRD). Furthermore, at high phosphate concentration, P removal percentage on Ca_2Al–Cl–LDH decreased in the order: pH 5.0 > pH 7.0 > pH 11.0. The reason for such a reduction of P removal efficiency was not yet clarified.

Herein, the study aimed to elucidate the phase structure of P–Al combination and the percentage of the constituents in precipitates formed at various pH values in the P removal on Ca_2Al–Cl–LDH. For this purpose, species of experimental precipitate was identified after P removal in the solution; the efficiency of Al and Ca in LDH on the P removal was also explored.

2. Materials and methods

2.1. Materials

Ca_2Al–Cl–LDH was prepared with a co-precipitation method as described previously [14]. In detail, at first, the salt solution (50 mL) was prepared by mixing two solutions of $CaCl_2$ (50 mmol) and $AlCl_3{\cdot}6H_2O$ (25 mmol). It was quickly added to the alkaline solution (100 mL), which contained 150 mmol of NaOH under acute stirring in high-purity nitrogen for 1 h.

After aging with continuous stirring at 25℃ for 18 h, the suspension subsequently passed through the filter. The precipitate was further washed and air dried at 100℃. For further test, the material was pressed and crushed (mesh size 100). The ICP and C/H/O element analysis further confirmed the purity of Ca_2Al–Cl–LDH, and the formula is $Ca_{1.8}Al(OH)_{5.6}Cl_{0.95}(CO_3)_{0.025}{\cdot}2.5H_2O$ (molecular weight is 275 g/mol). The XRD pattern of synthesized materials was consistent with previous research (JCPDS No 78-1219), and the d_{003}-spacing is 0.776 nm [10].

Pure P–Al precipitate was synthesized by precipitation, in which 3.086 g of $AlCl_3{\cdot}5H_2O$ was added to 300 mL of KH_2PO_4 solution ([P] = 1,000 mg/L) in a 500-mL beaker under vigorous stirring for 24 h. During this process, the pH value of the solution kept 4.0 constantly by NaOH or HNO_3 or solution (0.01 mmol/L). Finally, the precipitates were collected by centrifuge at 10,000 rpm for 15 min, followed by 80℃ drying in a vacuum oven.

2.2. Batch experiments

The phosphate removal was conducted in 100 mL KH_2PO_4 solution ([P] = 1,000 mg/L, 32.3 mmol/L) with 0.10 g dosage of Ca_2Al–Cl–LDH. The pH value in the solution was constant, respectively at 5.0, 7.0, and 11.0 throughout the experiment, adjusted by NaOH or HCl solution (0.01 mmol/L). The whole process of phosphate removal was performed at 25 ± 1℃, well shaken in the water bath for 24 h. At the end of the experiment, the suspension passed through 0.22 μm micropore membrane, and the solid was collected. After washing and air dried at 100℃, the solids and the solution was stored for further determination. Sample calcination was performed at 300, 700, and 860℃ for 8 h in a furnace, respectively. The calcined solids were milled for further characterization. Triplicates were conducted for all the experiments.

2.3. Chemical fractions of P from precipitate

For the three bulk samples, the phosphorous was extracted to identify the important host sites. By series of increasingly strong reagents to remove recalcitrant forms, various phosphorous was identified in accordance with previous method [6], modified by Williams et al. [15]. The phosphorous species included calcium phosphate (Ca-P), aluminum phosphate (Al-P), iron phosphate (Fe-P), and the occluded phosphate (O-P). More precisely, Ca-P was categorized as Ca_2-P (dicalcium phosphate), Ca_8-P (octacalcium phosphate), and Ca_{10}-P (10-calcium phosphate). After 0.2 g of solid sample was transferred into 100 mL flasks, the separation of each fractionation procedure was conducted at 20–25℃ with (1) 0.5 mol/L NH_4Ac (pH 4.2) for 1 h (Ca_2-P and Ca_8-P); (2) 0.1 mol/L NaOH and 0.05 mol/L Na_2CO_3 for 4 h (Al-P); and (3) 1.0 mol/L HCl for 1 h (Ca_{10}-P). Triplicates were conducted for all the experiments. Accordingly, the fraction of phosphorous bound to Ca was the total P in calcium phosphates extracted by NH_4Ac and HCl, whereas Al-associated phosphorous $AlPO_4$ extracted by NaOH–Na_2CO_3.

2.4. Chemical and physical characterization

The pH value was determined with the combined glass electrode (Model CL 51) by Elico digital pH meter (Model LI-120). The measurement of phosphate concentration followed the molybdenum blue colorimetric method, determined at 700 nm wavelength in a UNICO UV-spectrophotometer (4802UV/VIS). The metal concentrations were measured by the Inductively Coupled Plasma-Atom Emission Spectrometer (ICP-AES, Prodigy, Leeman Co.). The Element Analysis (EA3000, Leeman Co.) was introduced to detect the carbon, hydrogen, and oxygen components in LDH. The LDH was also analyzed by powder XRD on the D \MAX-2200 X-ray diffractometer (Rigaku Co.). The Cu Kα radiation ($\lambda = 0.15406$ nm) was employed with the scanning rate of 8°/min from 5° to 80° (2θ). The TG and DTA profiles of each sample were collected by the STA 449C thermo-gravimetric/differential thermal analyzer (TG/DTA, NETZSCH) in N_2 atmosphere at the ramping rate of 2℃/min from 30 to 900℃.

3. Results and discussion

3.1. Identification of $AlPO_4$ in synthesized P–Al precipitate

In our previous work [13], the theoretical phosphorous species in Ca_2Al–LDH precipitate was simulated by the PHREEQC program. It was reported that $AlPO_4$, $Ca_3(PO_4)_2$, and hydroxyapatite were the primary phosphorous precipitates at $pH \leq 7.0$, $7.0 < pH < 9.0$, and $pH \geq 9.0$, respectively. Although $AlPO_4$ was formed in simulation, it was not recognized by XRD in the experimental precipitate. To confirm the formation of $AlPO_4$ at $pH < 7.0$, the solid samples are calcined to crystallize the possible amorphous $AlPO_4$ phase. The proper temperature of the calcination was first obtained by TG/DTA analysis of synthesized $AlPO_4$.

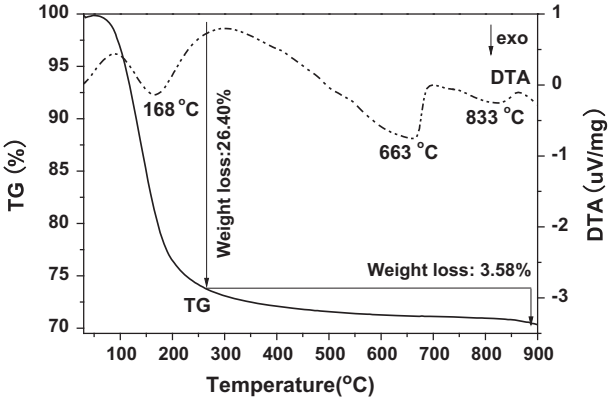

Fig. 1. TG/DTA curve of pure $AlPO_4$.

Fig. 1 illustrated the significant mass loss of 26.4% from 100 to 250℃ in the TG curve with an exothermal peak at 168℃ in DTA curve. This was attributed to the water loss on $AlPO_4$. For temperatures higher than 300℃, although the TG curve was relatively stable, there were two exothermal peaks at 663 and 833℃ detected by DTA, demonstrating two phase transition processes of pure P–Al precipitate.

Accordingly, $AlPO_4$ was calcined at 300, 700, and 860℃ for 8 h respectively to obtain the completed transition phase that could be identified by the XRD characterization. Fig. 2 shows the XRD pattern of amorphous $AlPO_4$ in the calcined sample before 300℃ as the broad peak at 15–40° (2θ). In contrast, well-crystallized $AlPO_4$ reflection was obtained in the XRD result of samples after calcination of 700℃. This suggested that the transition from amorphous to crystal $AlPO_4$ could be obtained after the calcination above 700℃. Moreover, the tridymite-like $AlPO_4$ (JCPDS No 51-1674) and quartz-like $AlPO_4$ (JCPDS No 11-0500) were predominant [16–18] after 700 and 860℃ calcination, respectively. This was consistent with the result of TG/DTA, indicated the phase transformation of tridymite-like $AlPO_4$ to quartz-like $AlPO_4$. This observation indicated that after the calcination at 860℃, the stable crystal $AlPO_4$ could be obtained. As a result, the calcination of the experimental precipitate was carried out at 860℃.

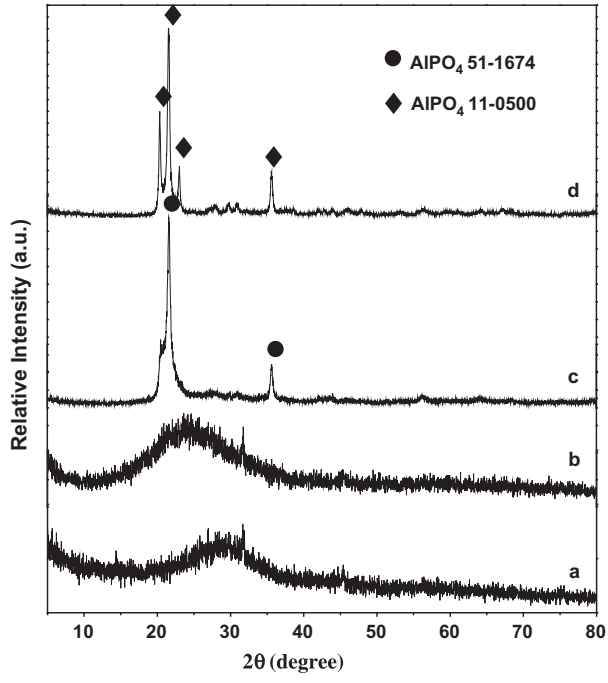

Fig. 2. XRD patterns of amorphous Al–P (a), calcined at 300℃ (b), 700℃ (c), and 860℃ (d).

3.2. Identification of $AlPO_4$ in experimental precipitate

Due to the complete dissolution of Ca_2Al–Cl–LDH, it was not observed in each precipitate after phosphorous removal, and there was no obvious pattern of $AlPO_4$ at pH 5.0 and 7.0. It was reported that in the presence of Al^{3+} in the acidic phosphate solution, a poor-crystallized $AlPO_4$ precipitate was formed with broad peak at 25–35° (2θ) [13]. Similarly for the treatment of pH 5.0, amorphous $AlPO_4$ was proposed in the current work. Furthermore, HAP was identified at pH 7.0, revealing that partial phosphorous was precipitated in HAP rather than DCPD, different from the results in simulation. It was worth noting that Al$(OH)_3$ was observed at pH 7.0 and 11.0, indicating no partial Al involved in the phosphorous precipitation.

However, as has been predicted, the calcined precipitate exhibited the formation of $AlPO_4$. As shown in Fig. 3, $Ca_3(PO_4)_2$ was observed in all calcined samples, which was due to the decomposition of hydrated P–Ca precipitate by high-temperature calcination. This accordingly suggested that there was hydrated P–Ca precipitate formed in the experimental precipitate, such as DCPD when the pH value was less than 7.0 and HAP at pH > 7.0. More importantly, the crystal $AlPO_4$ was identified predominantly in both calcined samples from precipitates when pH value was 5.0 and 7.0, indicating the transition of amorphous $AlPO_4$ to its crystal phase, which was similar to that in the case of synthesized $AlPO_4$. As a result, the amorphous $AlPO_4$ in the experimental precipitate at pH 5.0 and 7.0 was proposed.

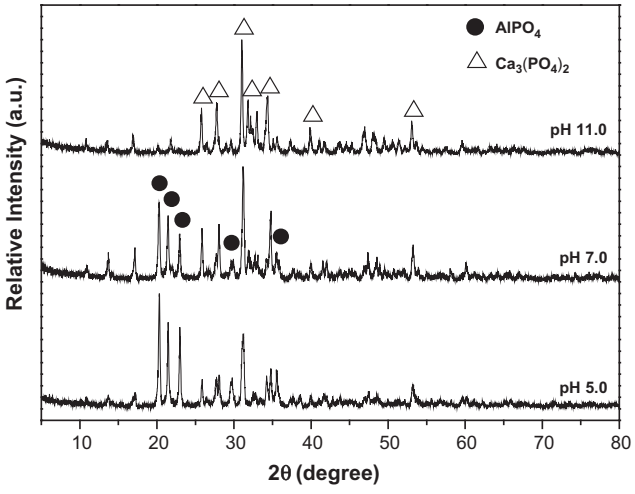

Fig. 3. XRD characterization of the calcined precipitate at 860 ℃.

3.3. The efficiency of Al and Ca in LDH on the P removal

Interestingly, the experimental composition of Ca and Al in the precipitate was estimated by phosphorous chemical extraction. As also listed in Table 1, the molar proportion of P–Al to total precipitate decreased from 56.6 to 5.80% with pH value increasing from 5.0 to 11.0. In the meanwhile, P–Ca value increased correspondingly to 94.2%. The results showed the similar molar ratio of (Ca + Al)/P at pH 5.0 in both experimental and simulated precipitate. However, the (Ca + Al)/P value in the experimental precipitate was not consistent with that of simulation at pH 7.0 and 11.0. The inconsistence of (Ca + Al)/P was contributed to the different evolution of Ca and Al precipitate between the experimental and simulated cases. For instance, HAP was identified at pH 7.0 [13], revealing that partial phosphorous was precipitated in HAP rather than DCPD, different from the results in simulation.

Furthermore, the concentration of Al ([Al]) left in solution after P removal increased with increasing pH. Specifically, [Al] at pH 5.0, of 2.13 mg/L suggested that 96.1 mg/g of Al in the precipitate due to 98.2 mg/g of total Al in LDH. The amount of P–Al was 110 mg/g as $AlPO_4$ was predominant in the precipitate (Fig. 3). This indicated that 56.6% of P removed was attributed to $AlPO_4$ precipitate.

In comparison, the efficiency of Al on P removal was limited at higher pH. At pH 7.0, there was 48 mg/g of P removed in $AlPO_4$ as 27.8% of P–Al in the solid sample. Accordingly, the amount of Al bond to P was 41.9 mg/g. On the other hand, [Al] was 6.20 mg/L in the solution, indicating 92 mg/g of total Al in the precipitate. This demonstrated that about 45% of Al contributed to P removal. The rest Al was in Al$(OH)_3$ formed in the precipitate according to the result of XRD (Fig. 2). Moreover, the efficiency of Al further decreased with increasing pH. At pH 11.0, the amount of Al in the precipitate was 49.5 mg/g, equilibrating 48.7 mg/L of Al in the solution. 49.6% of Al in the solution was attributed to the formation of soluble $Al(OH)_n^{-(n-3)}$ ($n > 3$) at higher pH [19]. As no $AlPO_4$ was observed in the precipitate, partial P was probably adsorbed on Al$(OH)_3$. This resulted in 5.80% of P associated with Al in the chemical extraction. Therefore, the contribution of Al to phosphorous removal was much higher under low-pH condition than that of high-pH environment.

The amount of P–Ca was 82, 125, and 121 mg/g when the pH value was 5.0, 7.0, and 11.0, respectively. Besides, the concentration of Ca ([Ca]) in the solution decreased from 145 to 0.16 mg/L with the increasing pH value, the residual [P] increased. The results indicated that the consumption of Ca increased as up to

Table 1
The proportion of P–Ca and P–Al contents in precipitates

	Theoretical		Practical						
pH	(Ca + Al)/P	Ca/P_{Ca}	[Al] (mg/L)	[Ca] (mg/L)	P–Al (%)	P–Ca (%)	(Ca + Al)/P	Ca/P_{Ca}	Residual P concentration (mmol/L)
5.0	1.02	1.00	2.13	145	56.6	43.4	1.05	1.10	26.1
7.0	1.01	1.00	6.20	29.4	27.8	72.2	1.48	1.44	26.7
11.0	2.41	1.67	48.7	0.16	5.80	94.2	2.21	1.68	26.9

99.9% of Ca in the precipitate due to 262 mg/g of total Ca in LDH, the removal efficiency of P decreased.

At pH 5.0, the molar ratio of Ca to P–Ca(Ca/P_{Ca}) was 1.10, similar to that of Ca/P in DCPD. The results showed that the consumed Ca was in DCPD form at acidic solution. The similar conclusion was also found when pH value was 11.0. The Ca/P_{Ca} was 1.68, close to 1.67 in the theoretical Ca/P simulation in HAP, showing that the consumed Ca was predominantly in HAP. Both observations were consistent with the results of XRD identification (Fig. 2).

In comparison, the Ca/P_{Ca} was 1.44 at pH 7.0, between those theoretical values of DCPD and HAP. This meant that both DCPD and HAP were formed in the collected sample. As a result, it was supposed that about 30% of consumed Ca was in DCPD and the rest in HAP. This observation suggested that the formation of HAP decreased the efficiency of Ca on P removal at basic solution.

4. Conclusions

The species of the precipitate after P removal in the solution was investigated. After the complete dissolution of LDH, Ca was precipitated in $CaHPO_4{\cdot}2H_2O$ (DCPD) at low pH while in hydroxyapatite (HAP) at relative high pH. For Al, amorphous $AlPO_4$ was predominant in the collected sample at pH 5.0, which was supported by the XRD result of the sample after thermal calcination. With pH increasing to 11.0, the formation of $Al(OH)_3$ was attributed to Al precipitation. Moreover, the chemical extraction and the concentration of ions in solution demonstrated that the consume efficiency of Al and Ca was higher at low pH than at high pH as the (Ca + .Al)/P increased from 1.05 to 2.21 with pH increasing. Accordingly, the formation of $AlPO_4$ and DCPD was inhibited at high pH, responsible for the reduction of P removal efficiency. Therefore, our result suggested that better P removal effect should be obtained in acidic solution on Ca_2Al–LDH as higher Al and Ca consume efficiency at low pH.

Acknowledgements

This project is financially supported by National Nature Science Foundation of China (Nos. 21107067/B070303 and 41472312/D0218), and Innovative Research Team in University (No. IRT13078). We also appreciate the technical support from Instrumental Analysis & Research Center of Shanghai University.

References

[1] J. Gao, Z. Xiong, J. Zhang, W. Zhang, F. Obono Mba, Phosphorus removal from water of eutrophic Lake Donghu by five submerged macrophytes, Desalination 242 (2009) 193–204.
[2] A. Montangero, H. Belevi, Assessing nutrient flows in septic tanks by eliciting expert judgement: A promising method in the context of developing countries, Water Res. 41 (2007) 1052–1064.
[3] S. Sengupta, A. Pandit, Selective removal of phosphorus from wastewater combined with its recovery as a solid-phase fertilizer, Water Res. 45 (2011) 3318–3330.
[4] C. Barca, C. Gérente, D. Meyer, F. Chazarenc, Y. Andrès, Phosphate removal from synthetic and real wastewater using steel slags produced in Europe, Water Res. 46 (2012) 2376–2384.
[5] H. Ratnaweera, H. Ødegaard, J. Fettig, Coagulation with prepolymerized aluminium salts and their influence on particle and phosphate removal, Water Sci. Technol. 26 (1992) 1229–1237.
[6] S. Chang, M.L. Jackson, Fractionation of soil phosphorus, Soil Sci. 84 (1957) 133–144.
[7] X. Chen, H. Kong, D. Wu, X. Wang, Y. Lin, Phosphate removal and recovery through crystallization of hydroxyapatite using xonotlite as seed crystal, J. Environ. Sci. 21 (2009) 575–580.
[8] S. Tanada, M. Kabayama, N. Kawasaki, T. Sakiyama, T. Nakamura, M. Araki, T. Tamura, Removal of phosphate by aluminum oxide hydroxide, J. Colloid Interface Sci. 257 (2003) 135–140.
[9] G. Qian, L. Feng, J.Z. Zhou, Y. Xu, J. Liu, J. Zhang, Z.P. Xu, Solubility product (Ksp)-controlled removal of chromate and phosphate by hydrocalumite, Chem. Eng. J. 181–182 (2012) 251–258.
[10] Y. Xu, Y. Dai, J. Zhou, Z.P. Xu, G. Qian, G.M. Lu, Removal efficiency of arsenate and phosphate from aqueous solution using layered double hydroxide materials: Intercalation vs. precipitation, J. Mater. Chem. 20 (2010) 4684–4691.

[11] A. Radha, P. Vishnu Kamath, C. Shivakumara, Mechanism of the anion exchange reactions of the layered double hydroxides (LDHs) of Ca and Mg with Al, Solid State Sci. 7 (2005) 1180–1187.
[12] S. Xu, Z. Chen, B. Zhang, J. Yu, F. Zhang, D.G. Evans, Facile preparation of pure CaAl-layered double hydroxides and their application as a hardening accelerator in concrete, Chem. Eng. J. 155 (2009) 881–885.
[13] J.Z. Zhou, L. Feng, J. Zhao, J. Liu, Q. Liu, J. Zhang, G. Qian, Efficient and controllable phosphate removal on hydrocalumite by multi-step treatment based on pH-dependent precipitation, Chem. Eng. J. 185–186 (2012) 219–225.
[14] U. Birnin-Yauri, F. Glasser, Friedel's salt, $Ca_2Al(OH)_6(Cl, OH)\cdot 2H_2O$: Its solid solutions and their role in chloride binding, Cem. Concr. Res. 28 (1998) 1713–1723.
[15] J. Williams, J. Syers, R. Harris, D. Armstrong, Fractionation of inorganic phosphate in calcareous lake sediments, Soil Sci. Soc. Am. J. 35 (1971) 250–255.
[16] I. Gregora, N. Magneron, P. Simon, Y. Luspin, N. Raimboux, E. Philippot, Raman study of $AlPO_4$ (berlinite) at the α–β transition, J. Phys.: Condens. Matter 15 (2003) 4487–4501.
[17] B.P. Onac, H.S. Effenberger, Re-examination of berlinite ($AlPO_4$) from the Cioclovina Cave, Romania, Am. Mineral. 92 (2007) 1998–2001.
[18] M. Youssif, F.S. Mohamed, M. Aziz, Chemical and physical properties of $Al_{1-x}Fe_xPO_4$ alloys, Mater. Chem. Phys. 83 (2004) 250–254.
[19] X. Yang, D. Wang, Z. Sun, H. Tang, Adsorption of phosphate at the aluminum (hydr)oxides–water interface: Role of the surface acid–base properties, Colloids Surf., A 297 (2007) 84–90.